Online Appendix for:
Asset Returns with Self-Exciting Jumps: Option Pricing and Estimation with a Continuum of Moments

H. Peter Boswijk*
Amsterdam School of Economics
University of Amsterdam
and Tinbergen Institute

Roger J. A. Laeven†
Amsterdam School of Economics
University of Amsterdam, EURANDOM
and CentER

Andrei Lalu‡
Amsterdam School of Economics
University of Amsterdam, Tinbergen Institute
and Duisenberg School of Finance

February 5, 2016

Abstract

This supplementary material contains finite sample identification considerations and computational aspects related to the estimation procedure we develop for the SVHJ model. Based on a Monte Carlo simulated data sample detailed in Section 1, we analyze in Section 2 the roles played by the various parameters of the SVHJ model in dictating the model-implied volatility surface and the associated way in which identification of the latent states is achieved. Next, based on the same simulated data sample, we analyze in Section 3 the sensitivity of the moment conditions to model parameters and the way in which parameter identification is achieved. An exposition of the numerical methods used to evaluate the moment conditions and the criterion function follows in Section 4. This appendix concludes in Section 5 with plots depicting the criterion function for the S&P 500 options data sample we consider in the paper.

*University of Amsterdam and Tinbergen Institute, P.O. Box 15867, 1001 NJ Amsterdam, The Netherlands. E-mail: H.P.Boswijk@uva.nl, Phone: +31 (0)20 5254252.

†University of Amsterdam, EURANDOM and CentER, P.O. Box 15867, 1001 NJ Amsterdam, The Netherlands. E-mail: R.J.A.Laeven@uva.nl, Phone: +31 (0)20 5254219.

‡University of Amsterdam, Tinbergen Institute and Duisenberg School of Finance, P.O. Box 15867, 1001 NJ Amsterdam, The Netherlands. E-mail: A.Lalu@uva.nl, Phone: +31 (0)20 5254245.

1 Simulated Data

In order to illustrate the numerical implementation of the estimation procedure we need to have a data sample available. For this purpose, we use a simulated state vector series and corresponding option panel data series generated following the approach detailed in the Monte Carlo design. The simulated state variable sample paths considered in this appendix consist of 500 observations sampled at weekly frequency ($\Delta = 5/250$). The parameter values used to generate the simulated sample are set at:

	$\mu_j^{\mathbb{P}}$	$\mu_j^{\mathbb{Q}}$	σ_j	η	κ_v	$\overline{v}$	σ_v	ρ	κ_λ	$\overline{\lambda}$	δ
True	-5%	-14%	6%	2.40	4.80	0.01	0.22	-0.60	18.00	0.5	10

Table 1: SVHJ model parameter values used to generate simulated data.

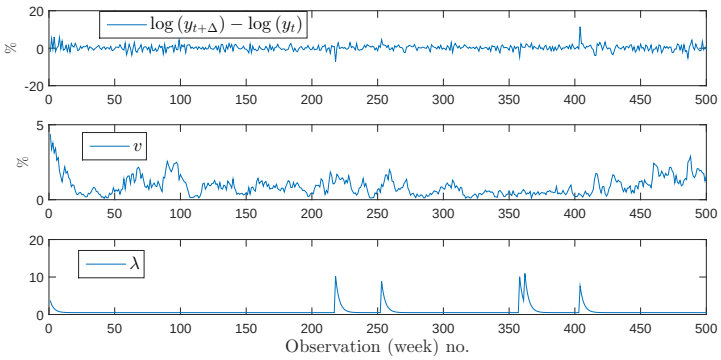

Figure 1: Plots of simulated state vector (y, v, λ) series ($n = 500$ time points, $\Delta = 5/250$, i.e., weekly data frequency).

2 Latent State Identification from Option Price Panels

2.1 Option Price Sensitivity to SVHJ Model Parameters

According to the SVHJ model specification outlined in the paper in Equations (2.11)–(2.13), the parameters in the $\mathbb{Q}$-measure specification of the model which appear in the option pricing routine are:

	Parameter	**Description**
1	$\mu_j^{\mathbb{Q}}$	jump size mean under $\mathbb{Q}$
2	σ_j	jump size standard deviation under $\mathbb{P}$ and $\mathbb{Q}$
3	κ_v	speed of stoch. vol. mean reversion
4	$\overline{v}$	long run mean of stoch. vol.
5	σ_v	volatility of the stoch. vol.
6	ρ	leverage between stoch. vol. and returns
7	κ_λ	speed of self-exciting jump intensity mean reversion
8	$\overline{\lambda}$	self-exciting jump intensity long run mean
9	δ	self-exciting jump intensity jump size

Table 2: Overview of SVHJ model parameters.

Each of the parameters influences the shape of the Black-Scholes implied volatility surface resulting from model-generated prices. Figure 2 depicts this in a numerical example. The profile of the implied volatility surface can be described in terms of the skew and slope

it has in different regions of money-ness and maturity. For equity options, the skew[1] is known to vary with maturity (T), whereas the overall direction of the slope depends on the current level of instantaneous volatility compared to its long run level towards which it mean reverts. Table 3 summarizes the predominant contribution of each SVHJ model parameter with regards to the shape of the implied volatility surface:

IV surface feature	**Parameters with predominant impact**
Skew for short term-to-maturity:	$\mu_j^{\mathbb{Q}}$, $\sigma_j^{\mathbb{Q}}$;
Skew for all maturities:	$\sigma_v, \rho, \kappa_\lambda, \delta$;
Slope:	(nonlinear:) $\kappa_v, \kappa_\lambda, \delta$; (approx. linear:) $\overline{v}, \overline{\lambda}$;

Table 3: Impact of SVHJ model parameters on the Black-Scholes implied volatility surface features.

Note that each of the implied volatility surface profile characteristics is jointly influenced by several parameters. The impact of each parameter is enhanced or attenuated by the level of the state variables whose dynamics it determines.[2] Therefore, the fact that the volatility state variable is more persistent than the jump intensity state variable plays an important role in disentangling the contribution of each parameter as the dynamics of the surface changes over time. In other words, parameter identification would likely only be possible when taking into account the dynamics of the implied volatility surface over time, particularly over periods in which jumps occur. A "static" calibration exercise is unlikely to be able to identify SVHJ model parameters, as the impact of the jump intensity related parameters would be hard to distinguish from the impact of (some) of the stochastic volatility related parameters.

The parameters characterizing the jump size distribution have a strong isolated impact on the short term maturity skew, suggesting that they have a predominant role in explaining smirk shapes, particularly during turbulent times, when the jump intensity state variable is large.

Sudden shifts followed by quick reversals in the level and skew of the implied volatility surface (e.g., such episodes are frequent during turbulent market episodes) are the subset of the option price time series which contributes to the identification of the jump intensity parameters. The intuition behind the identification strategy is that it requires tracking the shifts in the implied volatility surface during turbulent times when jumps take a predominant role in governing its dynamics.

The parameters describing the stochastic volatility process dynamics together with the long run mean of the jump intensity (i.e., $\overline{\lambda}$) are pinned down by the long run dynamics of the implied volatility surface.

The Monte Carlo results presented in Section 3.3 of the paper confirm that this identification strategy performs well in finite samples.

2.2 Backing Out Latent States from Option Prices

To back out discrete time observations on the level of the two latent stochastic states we use a non-linear least squares type of minimization procedure at each sample time point to recover the state levels which would render the best fit for a pre-selected grid of SVHJ model-based option prices compared to their market observed counterparts. The details of this procedure are presented in Section 3.1 of the paper.

Figure 3 shows how the latent states depend on model parameters (the dependence is depicted by varying one parameter, while the remaining parameters are set equal to the values used to simulate the state variable series and the corresponding option prices).

We observe that backing out the latent states using parameter values which do not correspond to their true values yields distorted states, particularly at the time points following jump events.

[1] The shape of the skew for equity options with small maturities is often referred to as a "smirk".

[2] This effect goes through the conditional characteristic function which is used in the option pricing routine.

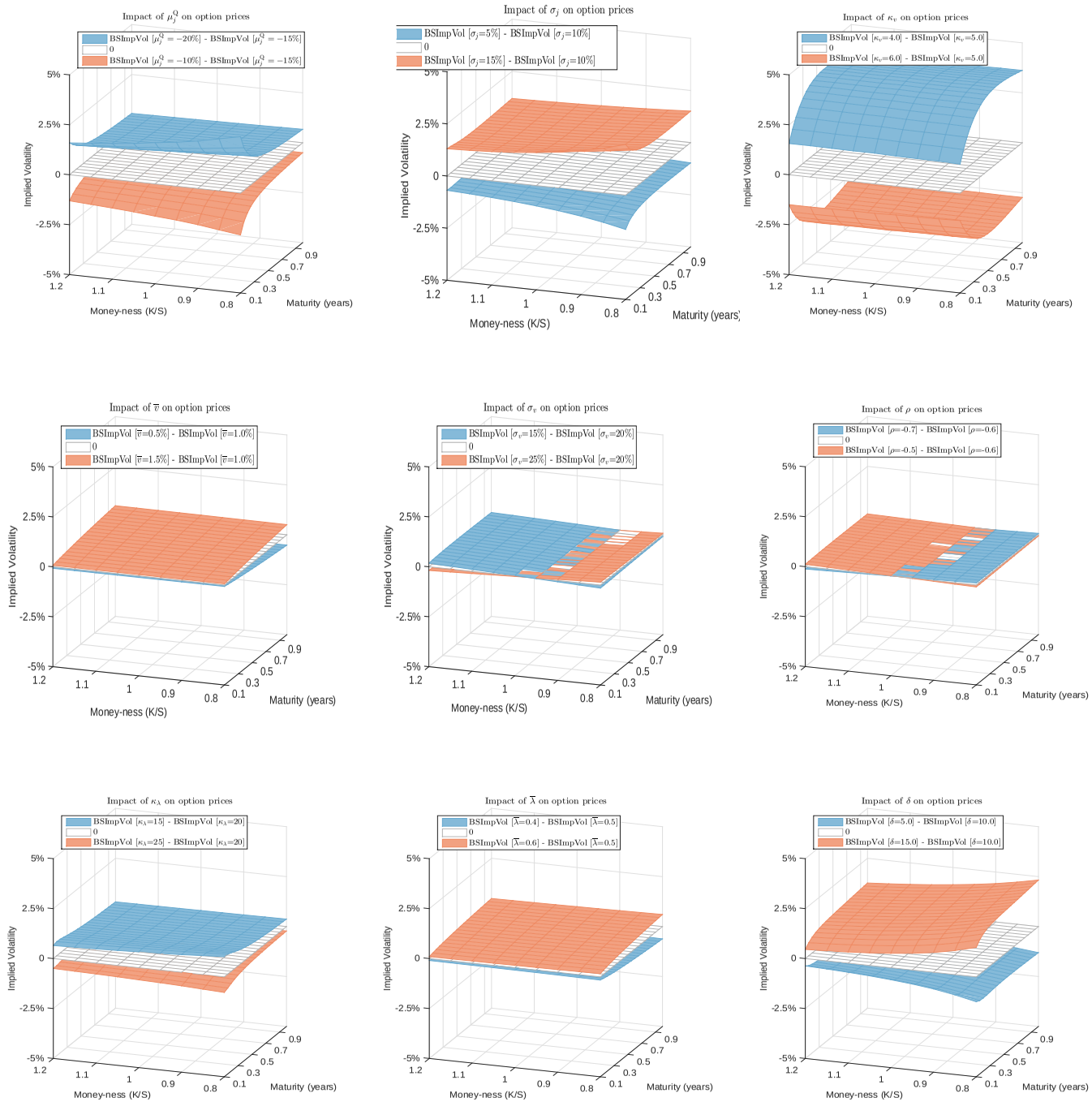

Figure 2: Parameter-by-parameter plots depicting the impact which each model parameter has on the option-implied volatility surface (i.e., the influence which parameter variations have on option prices). In each of the sub-figures one of the parameters is varied while keeping the remaining parameters fixed.

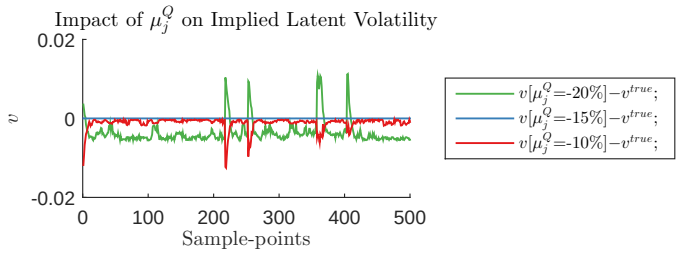
Impact of μ_j^Q on Implied Latent Volatility
$v[\mu_j^Q$=-20%$]-v^{true}$;
$v[\mu_j^Q$=-15%$]-v^{true}$;
$v[\mu_j^Q$=-10%$]-v^{true}$;
Sample-points

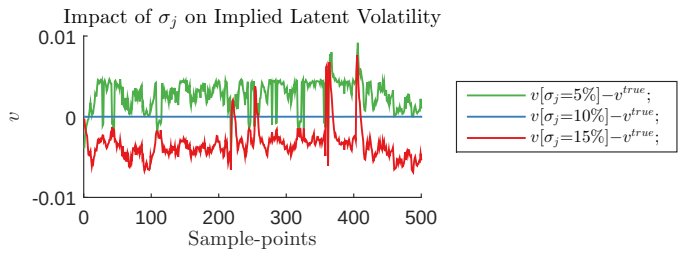
Impact of σ_j on Implied Latent Volatility
$v[\sigma_j$=5%$]-v^{true}$;
$v[\sigma_j$=10%$]-v^{true}$;
$v[\sigma_j$=15%$]-v^{true}$;
Sample-points

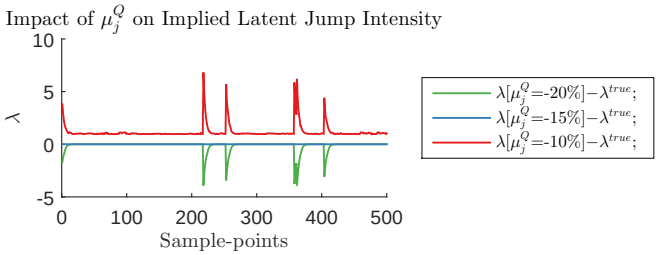
Impact of μ_j^Q on Implied Latent Jump Intensity
$\lambda[\mu_j^Q$=-20%$]-\lambda^{true}$;
$\lambda[\mu_j^Q$=-15%$]-\lambda^{true}$;
$\lambda[\mu_j^Q$=-10%$]-\lambda^{true}$;
Sample-points

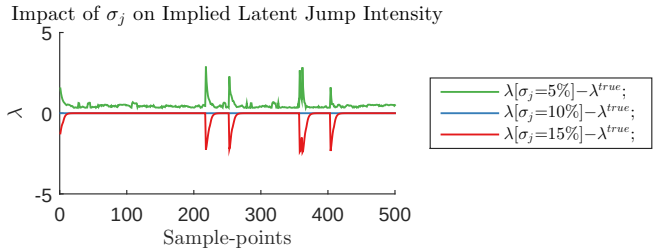
Impact of σ_j on Implied Latent Jump Intensity
$\lambda[\sigma_j$=5%$]-\lambda^{true}$;
$\lambda[\sigma_j$=10%$]-\lambda^{true}$;
$\lambda[\sigma_j$=15%$]-\lambda^{true}$;
Sample-points

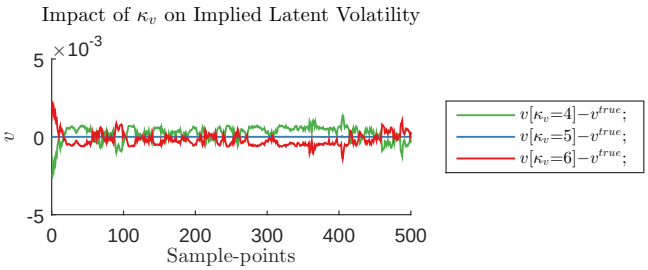
Impact of κ_v on Implied Latent Volatility
$v[\kappa_v$=4$]-v^{true}$;
$v[\kappa_v$=5$]-v^{true}$;
$v[\kappa_v$=6$]-v^{true}$;
Sample-points

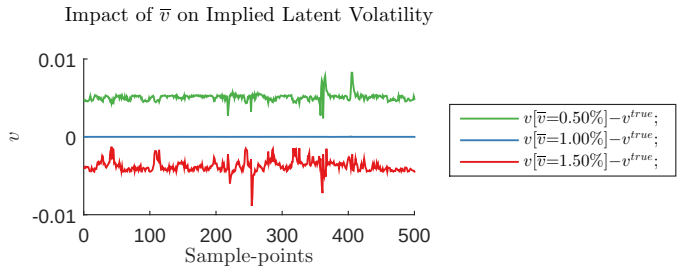
Impact of $\overline{v}$ on Implied Latent Volatility
$v[\overline{v}$=0.50%$]-v^{true}$;
$v[\overline{v}$=1.00%$]-v^{true}$;
$v[\overline{v}$=1.50%$]-v^{true}$;
Sample-points

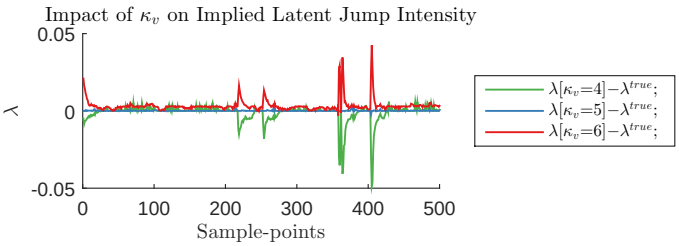
Impact of κ_v on Implied Latent Jump Intensity
$\lambda[\kappa_v$=4$]-\lambda^{true}$;
$\lambda[\kappa_v$=5$]-\lambda^{true}$;
$\lambda[\kappa_v$=6$]-\lambda^{true}$;
Sample-points

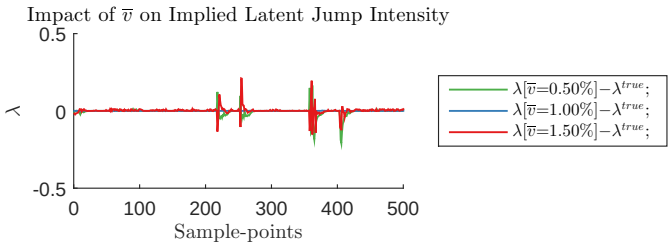
Impact of $\overline{v}$ on Implied Latent Jump Intensity
$\lambda[\overline{v}$=0.50%$]-\lambda^{true}$;
$\lambda[\overline{v}$=1.00%$]-\lambda^{true}$;
$\lambda[\overline{v}$=1.50%$]-\lambda^{true}$;
Sample-points

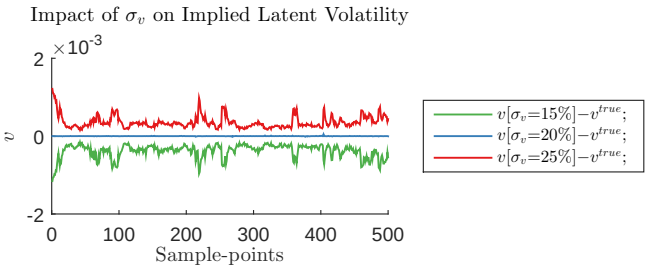
Impact of σ_v on Implied Latent Volatility
$v[\sigma_v$=15%$]-v^{true}$;
$v[\sigma_v$=20%$]-v^{true}$;
$v[\sigma_v$=25%$]-v^{true}$;
Sample-points

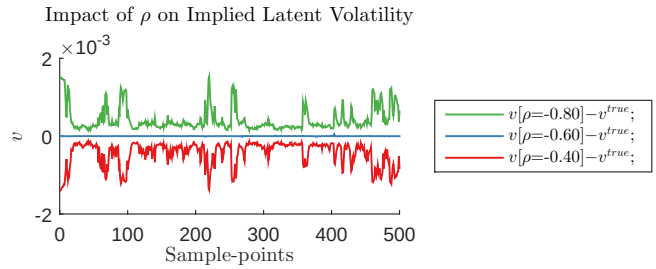
Impact of ρ on Implied Latent Volatility
$v[\rho$=-0.80$]-v^{true}$;
$v[\rho$=-0.60$]-v^{true}$;
$v[\rho$=-0.40$]-v^{true}$;
Sample-points

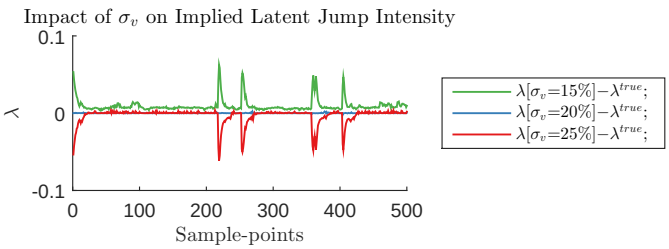
Impact of σ_v on Implied Latent Jump Intensity
$\lambda[\sigma_v$=15%$]-\lambda^{true}$;
$\lambda[\sigma_v$=20%$]-\lambda^{true}$;
$\lambda[\sigma_v$=25%$]-\lambda^{true}$;
Sample-points

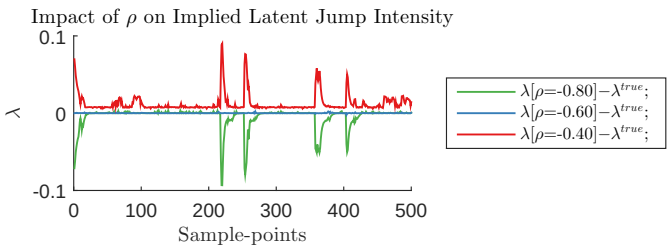
Impact of ρ on Implied Latent Jump Intensity
$\lambda[\rho$=-0.80$]-\lambda^{true}$;
$\lambda[\rho$=-0.60$]-\lambda^{true}$;
$\lambda[\rho$=-0.40$]-\lambda^{true}$;
Sample-points

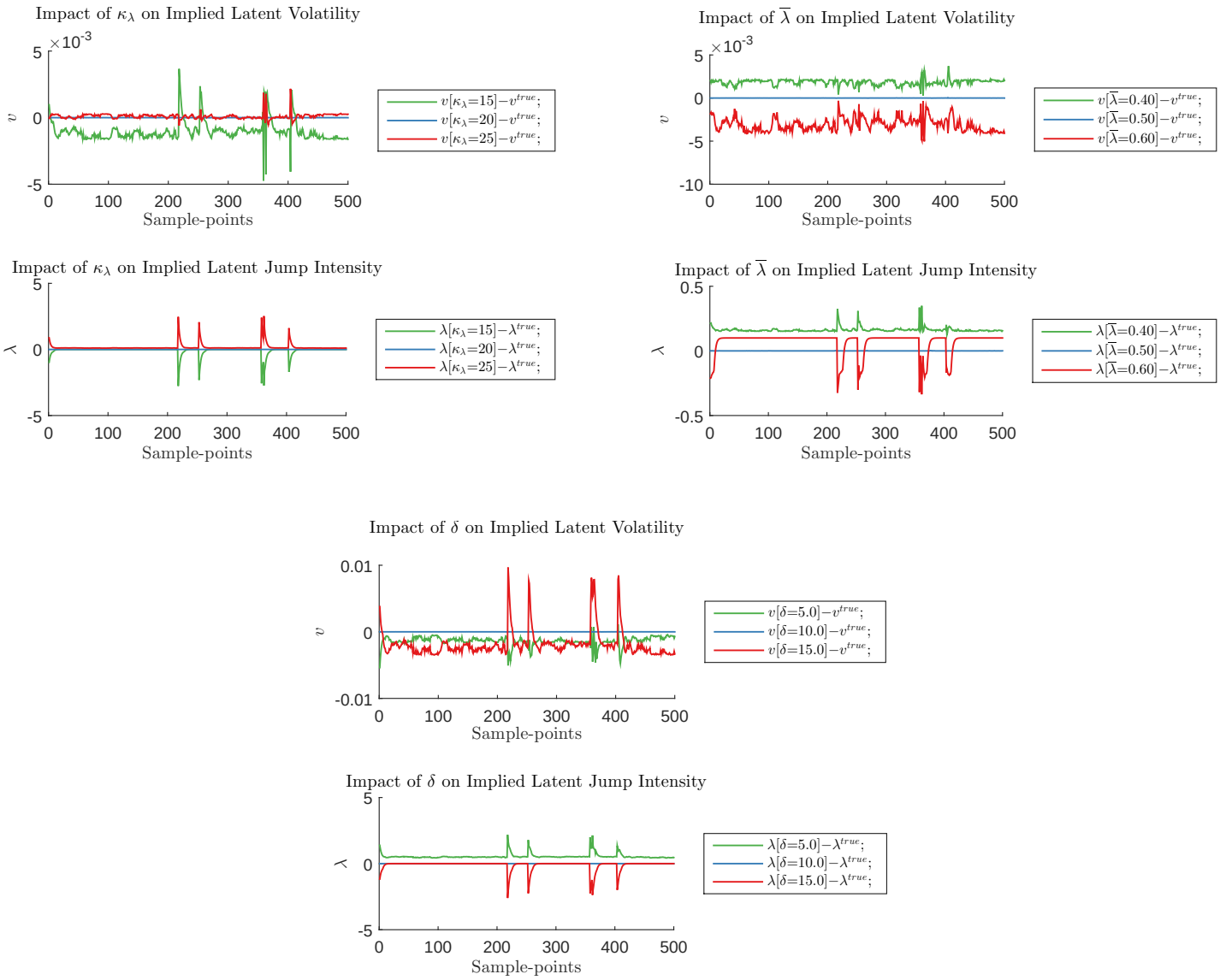

Figure 3: The plots show the sensitivity of the backed out latent states with respect to each of the SVHJ model parameters. In each plot, one of the parameters is varied while all the other parameters are set equal to their true values (given in Table 1). The lines plot the difference between the "true" value of the latent state and its backed out value. In all cases the "true" values of the latent states can be backed out subject to an arbitrarily small numerical error when using the true parameter vector (i.e., blue line coincides with the zero-line). The green and red lines show the difference between the backed out state and its true values when parameters deviate from "true" values used to simulate the state vector sample series.

3 Moment Conditions

The moment condition expressions depend on the parameter vector θ explicitly through the evaluations of the conditional characteristic function $\phi(s, X_{t_i}^{\theta}, \Delta; \theta)$ and implicitly through the backed out latent states $X_{t_i}^{\theta} = \left[y_{t_i}, v_{t_i}^{\theta}, \lambda_{t_i}^{\theta}\right]$. Therefore, the moment conditions in our proposed set-up with latent states backed out from option prices are intricate functions of the parameter vector. Before looking at an example which shows the sensitivity of the moment conditions with respect to the parameters, we first point out the need to re-scale the state vector so as to facilitate further numerical analysis.

3.1 State Variable Re-Scaling. Marginal Conditional Characteristic Functions

To depict the way in which the conditional characteristic function depends on the parameters, consider analyzing the marginals of the conditional characteristic function for each of the three state variables in the SVHJ model (under the physical probability measure $\mathbb{P}$):

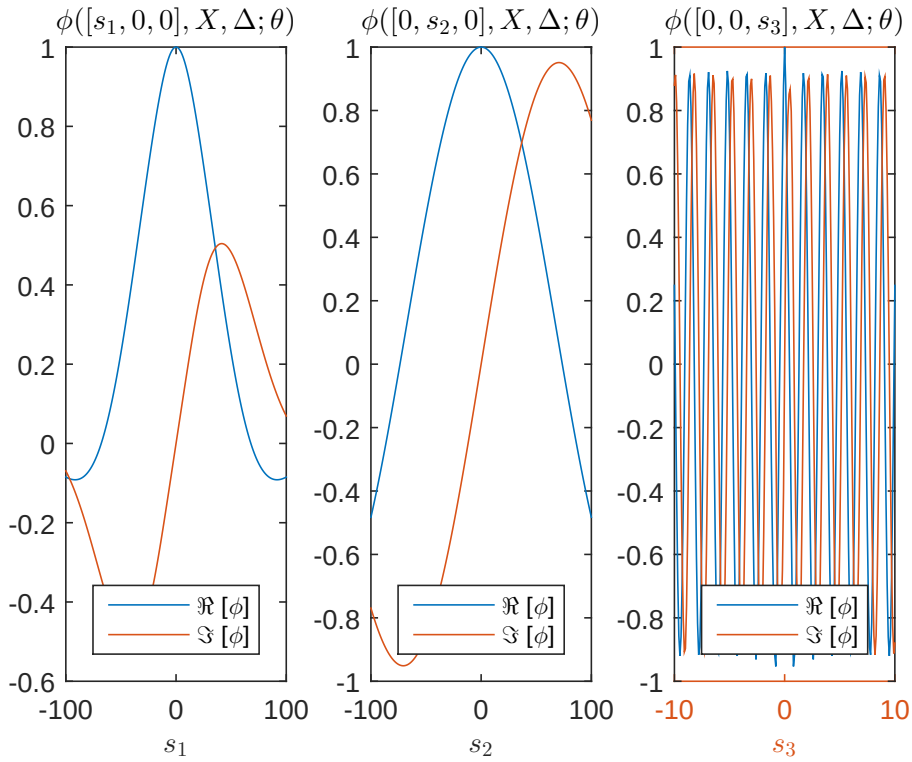

Figure 4: Real and imaginary parts of the marginal conditional characteristic functions. The state vector is set at $X = [0.01, 0.15^2, 5]$. The time step is set accordingly for a weekly data frequency, i.e., $\Delta = 5/250$. θ is set at the values given in Table 1.

Notice that the marginal conditional characteristic function for the stochastic jump intensity variable has a pronounced oscillatory behavior. This behavior poses difficulties for the numerical integration required to evaluate the criterion function. In our initial simulations, the precision of the estimator based on the conditional characteristic function of the self-exciting jump process was sensitive to the choice of quadrature scheme used for the integral approximation. To address this numerical issue, we propose re-scaling the jump intensity state variable and the corresponding parameters accordingly, while maintaining the same jump dynamics in the model.

The dynamics of the re-scaled jump intensity state $\lambda_t^{\star} \equiv c \times \lambda_t, c \in \mathbb{R}^*$ lead to definitions

of re-scaled self-exciting jump intensity parameters, i.e.:

$$\begin{aligned}
\mathrm{d}(c \times \lambda) &= c \times \kappa_\lambda \left(\overline{\lambda} - \lambda_t\right) \mathrm{d}t + c \times \delta \, \mathrm{d}N_t \Rightarrow \\
\mathrm{d}(\lambda_t^\star) &= \kappa_\lambda \left(c \times \overline{\lambda} - \lambda_t^\star\right) \mathrm{d}t + c \times \delta \, \mathrm{d}N_t \\
&= \kappa_\lambda \left(\overline{\lambda}^\star - \lambda_t^\star\right) \mathrm{d}t + \delta^\star \, \mathrm{d}N_t,
\end{aligned}$$

where $\overline{\lambda}^\star \equiv c \times \overline{\lambda}$ and $\delta^\star \equiv c \times \delta$.

The re-scaled stochastic jump intensity $\lambda_t^\star$ is scaled back when used to describe the $\mathcal{F}_t$-conditional instantaneous mean jump rate of N_t per unit of time, i.e.:

$$\begin{cases}
\mathbb{P}\left[N_{t+\Delta} - N_t = 0 | \mathcal{F}_t\right] = 1 - \frac{1}{c}\lambda_t^\star \Delta + o(\Delta); \\
\mathbb{P}\left[N_{t+\Delta} - N_t = 1 | \mathcal{F}_t\right] = \frac{1}{c}\lambda_t^\star \Delta + o(\Delta); \\
\mathbb{P}\left[N_{t+\Delta} - N_t > 1 | \mathcal{F}_t\right] = o(\Delta);
\end{cases} \tag{3.1}$$

with $\Delta > 0$ a small time step. Therefore the conditional probabilities of jump events are not affected by the re-scaling procedure, i.e., the model dynamics are not changed as a result of the re-scaling.

The marginal conditional characteristic function of the re-scaled variable is noticeably easier to integrate within the domain considered. We remark that the marginal conditional characteristic functions of the remaining states are unaffected by the re-scaling:

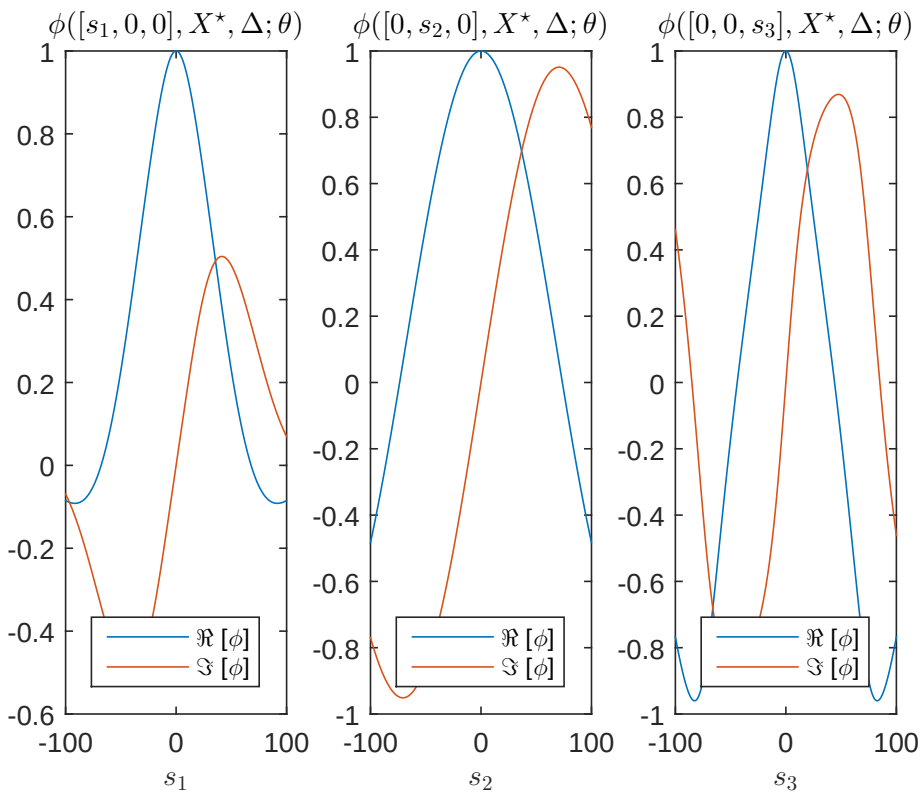

Figure 5: Re-scaled marginal conditional characteristic functions evaluated in the range $[-100, 100]$. The state vector is set at $X = [0.01, 0.15^2, 5/c]$. The time step is set accordingly for a weekly data frequency, i.e., $\Delta = 5/250$. θ is set at the values given in Table 1, with the values corresponding to $\overline{\lambda}$ and δ replaced with the corresponding $\overline{\lambda}^\star \equiv c \times \overline{\lambda}$ and $\delta^\star \equiv c \times \delta$. In this example, the scaling parameter was set to $c = 100$.

3.2 Moment Function - Parameter Sensitivity

This subsection analyzes the sensitivity of the moment conditions with respect to the parameters, taking into account the full picture in which the implied latent states also depend on the value of the parameters. Figure 6 plots examples of sample average moment conditions based on the conditional characteristic function for the simulated sample, with the state vector levels implied from option prices. Each subplot shows either the real or the imaginary part of the sample average for a moment condition based on one of the marginal conditional characteristic functions of the model state variables. The criterion function integrates over (the square) of similar[3] moment conditions. Note that in most subplots the integral which would correspond to the moment condition evaluated at the true parameter values (middle value in each of the plots) would be the smallest, indicative of the way in which parameter identification is achieved.

[3]The actual moment conditions used in the estimation procedure concern the conditional characteristic function of the entire state vector (not only the marginals) and are weighted with Gaussian weights. The marginals are shown here for illustrative purposes.

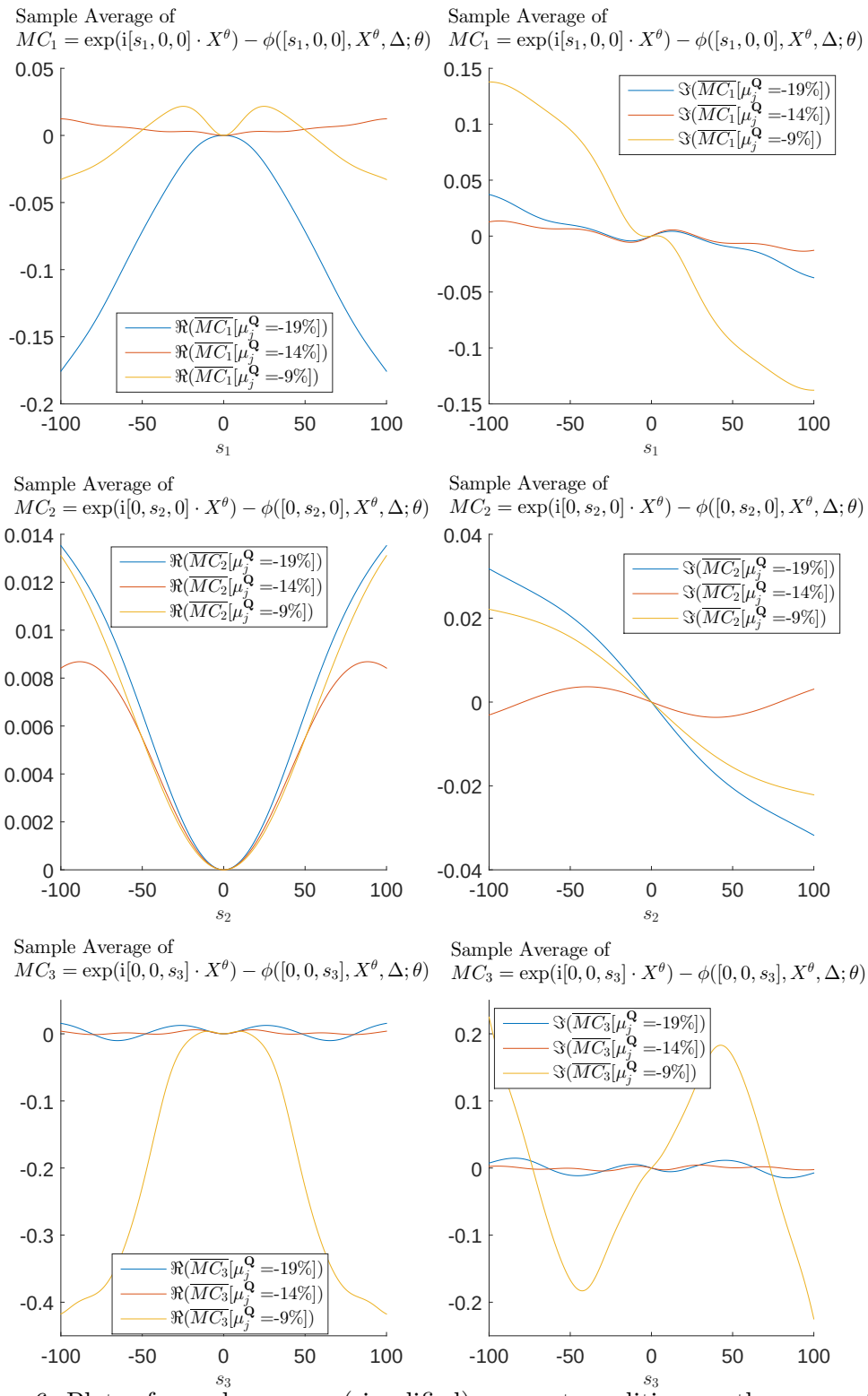

Figure 6: Plots of sample average (simplified) moment conditions as the parameter corresponding to the mean jump size under $\mathbb{Q}$ is varied. $\Re(\overline{MC})$ and $\Im(\overline{MC})$ denote the real and imaginary parts, respectively, of the (simplified) moment condition functions. The moment conditions depend explicitly on this parameter through the conditional characteristic function and implicitly through the latent implied stochastic volatility $v_{t_i}^\theta$ and latent implied stochastic jump intensity $\lambda_{t_i}^\theta$. Note that the sample averages of the moment conditions corresponding to $\mu_j^{\mathbb{Q}} = 14\%$, which is the true value used to simulate the data-set, typically have the smallest absolute value.

4 Numerical Evaluation of the Criterion Function

4.1 Multivariate Integral - Numerical Evaluation Approaches

Evaluating the criterion function entails the computation of a multi-dimensional integral with Gaussian weights over the Euclidean space. The dimension of the integration domain for which numerical procedures are required can be "halved" by analytically integrating out the instruments from the criterion function. As shown in [Carrasco et al., 2007a] (repeated here using our notation for the reader's convenience):

$$
\begin{aligned}
&\int_{\tau\in\mathbb{R}^{p\times 2}} \hat{h}_n(\tau;\theta)\overline{\hat{h}_n(\tau;\theta)}\pi(\tau)\,\mathrm{d}\tau = \\
&= \int_{s\in\mathbb{R}^p}\int_{r\in\mathbb{R}^p} \frac{1}{(n-1)^2}\left[\sum_{i=1}^{n} e^{\mathrm{i}r\cdot X^\theta_{t_i}}\left(e^{\mathrm{i}s\cdot X^\theta_{t_{i+1}}} - \phi(s, X^\theta_{t_i}, \Delta;\theta)\right)\right] \\
&\qquad\qquad \times \left[\sum_{j=1}^{n} \overline{e^{\mathrm{i}r\cdot X^\theta_{t_j}}\left(e^{\mathrm{i}s\cdot X^\theta_{t_{j+1}}} - \phi(s, X^\theta_{t_j}, \Delta;\theta)\right)}\right]\pi(r)\pi(s)\,\mathrm{d}r\,\mathrm{d}s \\
&= \frac{1}{(n-1)^2}\int_{s\in\mathbb{R}^p}\sum_{i=1}^{n}\sum_{j=1}^{n}\left[\left(\int_{r\in\mathbb{R}^p} e^{\mathrm{i}r\cdot\left(X^\theta_{t_i}-X^\theta_{t_j}\right)}\pi(r)\,\mathrm{d}r\right)\right. \\
&\qquad \left.\times\left(e^{\mathrm{i}s\cdot X^\theta_{t_{i+1}}} - \phi(s, X^\theta_{t_i}, \Delta;\theta)\right)\left(e^{-\mathrm{i}s\cdot X^\theta_{t_{i+1}}} - \phi(-s, X^\theta_{t_i}, \Delta;\theta)\right)\right]\pi(s)\,\mathrm{d}s \\
&= \frac{1}{(n-1)^2}\int_{s\in\mathbb{R}^p}\sum_{i=1}^{n}\sum_{j=1}^{n}\left[\exp\left(\frac{-(X^\theta_{t_i}-X^\theta_{t_j})^\top\Sigma_r(X^\theta_{t_i}-X^\theta_{t_j})}{2}\right)\right. \\
&\qquad \left.\times\left(e^{\mathrm{i}s\cdot X^\theta_{t_{i+1}}} - \phi(s, X^\theta_{t_i}, \Delta;\theta)\right)\left(e^{-\mathrm{i}s\cdot X^\theta_{t_{i+1}}} - \phi(-s, X^\theta_{t_i}, \Delta;\theta)\right)\right]\pi(s)\,\mathrm{d}s.
\end{aligned}
$$

The above simplification is due to the analytic solution:

$$
\int_{r\in\mathbb{R}^p} e^{\mathrm{i}r\cdot\left(X^\theta_{t_i}-X^\theta_{t_j}\right)}\pi(r)\,\mathrm{d}r = \exp\left(\frac{-(X^\theta_{t_i}-X^\theta_{t_j})^\top\Sigma_r(X^\theta_{t_i}-X^\theta_{t_j})}{2}\right),
$$

where Σ_r denotes the diagonal covariance matrix of the of vector coordinates r at which the instrument expression $m(r, X_{t_i}) = e^{\mathrm{i}r\cdot X_{t_i}}$ is evaluated.

Note that the remaining integration problem has the same dimension as the state vector, therefore the above calculation yields a dimension reduction which eases the computational effort required to evaluate the criterion function. In the SVHJ model set-up, the estimation routine requires successive evaluations of an integral over the 3-dimensional Euclidean space ($\dim X = 3$) with the Gaussian weight function, $\pi(s), s \in \mathbb{R}^3$.

Quadrature methods

A survey of classical numerical methods for the evaluation of high-dimensional integrals can be found in Chapter 3 of [Holtz, 2011]. In contexts with moderate integrand dimensions, such as the 3-dimensional case arising in our SVHJ model estimation procedure, a wide range of feasible numerical approaches is readily available for obtaining quadrature-based approximations of the integral.

Quadrature methods approximate the value of a d-dimensional integral $I = \int_{\mathbb{R}^d} f(s)\,\mathrm{d}s$ of an integrable function $f(s), f : \mathbb{R}^d \to \mathbb{R}$ by a weighted sum of a finite, typically small number of function evaluations:

$$
I_n = \sum_{i=1}^{n} \omega_i f(s_i),
$$

where $\omega_i \in \mathbb{R}$ denotes a scalar weight and $s_i \in \mathbb{R}^d, i = 1, \ldots, n$ denotes the evaluation point. Different choices of evaluation points and weights distinguish different classes of evaluation methods.

Monte Carlo approximation methods rely on a Law of Large Numbers result and presuppose using equal weights, e.g., $\omega_i = \frac{1}{n}$, and uniformly distributed draws for the sequence $\{s_i\}$ of evaluation points. As it relies on a probabilistic convergence rate, this integral evaluation method typically requires many function evaluations which would become computationally expensive in the SVHJ estimation context in which we also rely on numerical ODE solvers for integrand evaluation.

It is more cost efficient computational-wise to evaluate the criterion function integral in the SVHJ set-up by using multivariate extensions of (univariate) quadrature rules. Univariate quadrature rules are pre-determined (fixed) sets of weights and evaluation points used to approximate integrals over the (one-dimensional) Euclidean space $\mathbb{R}$ or over the unit interval $[0, 1]$ spaces. Through various combinations of tensor products, the univariate quadrature rules for integrals with Gaussian weights such as Gauss-Hermite formulas have been extended to multivariate integration domains. We utilize the Matlab routine *fwtpts* provided by [Genz], to obtain points and weights for 3-dimensional integration using the [Genz and Keister, 1996] quadrature rules. Figure 7 shows a typical set of 3-dimensional quadrature points. Note that, for example, a rule suitable for the evaluation of integrands which could be represented by polynomials with degree of up to 11, all quadrature point coordinates are in the $[-5, 5]$ range. This limited range emphasizes that it is important to re-scale the state variables (in the SVHJ set-up in particular - the jump intensity state) such that the response of the conditional characteristic function to parameter changes can be captured within the range of integrand evaluation points.

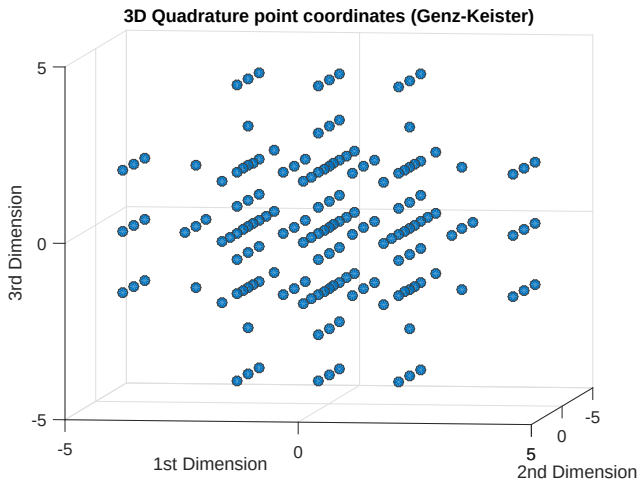

Figure 7: Typical set of 3-dimensional quadrature points.

5 Criterion Function Convergence Plots

Finally, this appendix presents plots depicting the values of the second step criterion function in the neighborhood of the parameter estimates for the (in-sample part) of the data set containing S&P 500 option prices used in the paper. The plots show the profile of the second step criterion function as one parameter estimate varies while remaining parameters are fixed at estimated values.

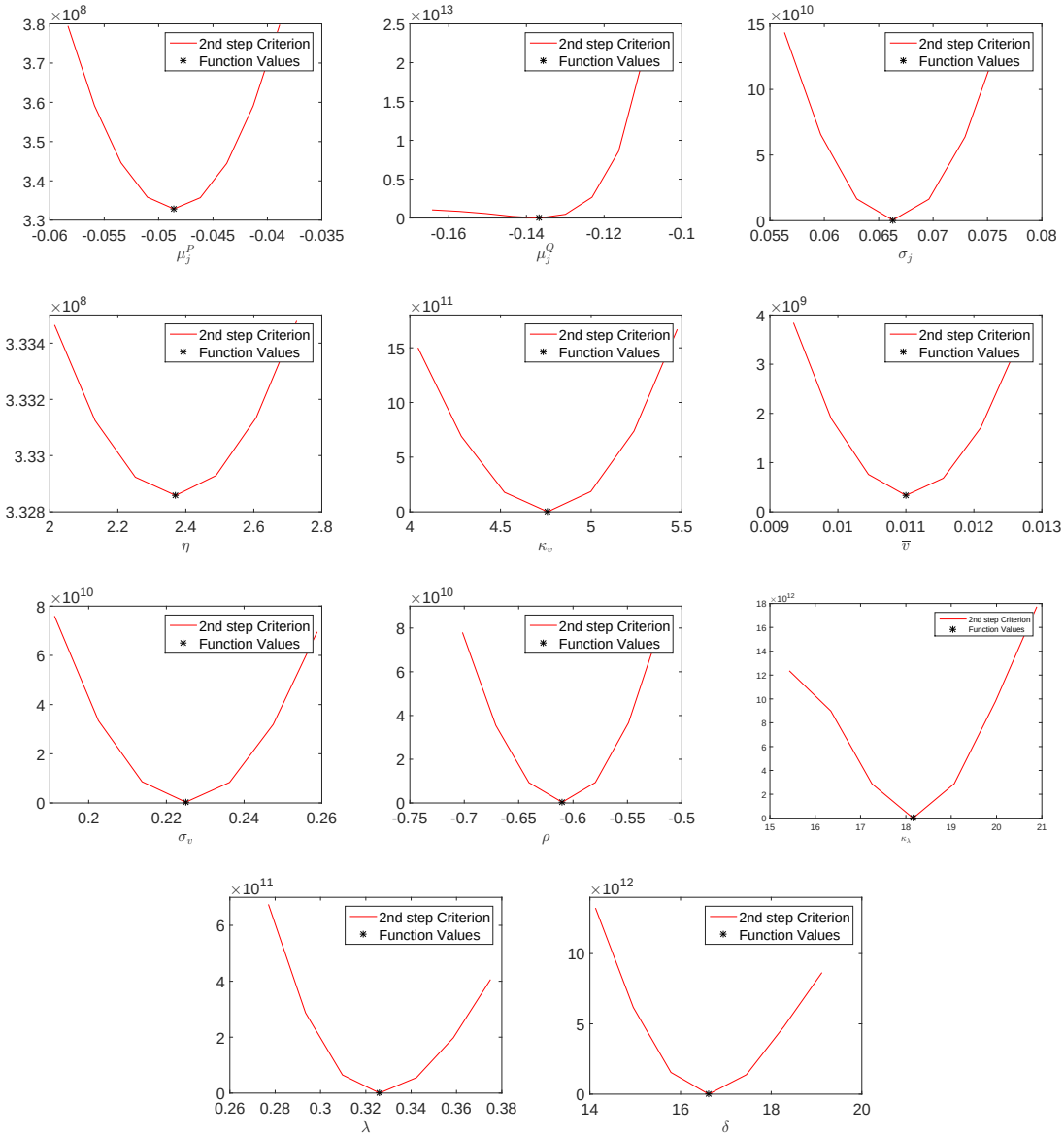

Figure 8: Parameter-by-parameter plots depicting the profile of the 2nd step criterion function for the data sample used in the estimation. Each figure plots the criterion function as one of the parameters varies and remaining ones are fixed at estimated values.

References

[Carrasco et al., 2007a] Carrasco, M., Chernov, M., Florens, J.-P., and Ghysels, E. (2007a). Efficient estimation of general dynamic models with a continuum of moment conditions. *Journal of Econometrics*, 140(2):529–573.

[Genz] Genz, A. A Matlab function with supporting functions, for the computation of points and weights for fully symmetric interpolatory rules (these are sparse-grid rules) for integration over hyper-cubes or Gaussian weighted hyperspace. `http://www.math.wsu.edu/faculty/genz/software/matlab/fwtpts.m`. Accessed November 2014.

[Genz and Keister, 1996] Genz, A., and Keister, B. (1996). Fully symmetric interpolatory rules for multiple integrals over infinite regions with Gaussian weight. *Journal of Computational and Applied Mathematics*, 71:299–309.

[Holtz, 2011] Holtz, M. (2011). *Sparse grid quadrature in high dimensions with applications in finance and insurance*. Vol. 77, Springer Science & Business Media.